A Generalised Block Diagram Model for Small-Signal Stability Analysis of Multi-machine, Multi-SVC Power Systems

Pichai Aree
Department of Electrical Engineering, Faculty of Engineering,
Thammasat University, Pathumthani, 12121, Thailand.

Abstract

This paper introduces a newly extended transfer function block diagram model which accommodates *n* synchronous generators and *m* SVC systems in a single frame-of-reference. The new simulation environment is used to conduct fundamental studies of dynamic interactions between synchronous generators and between synchronous generators and SVC systems. This method yields physical insight and differs from the well-known state-space techniques. The system model includes the full dynamic representation of synchronous machines in terms of field and damper windings in *d*- and *q*-axes. The small-signal dynamic performance of various system models, incorporating a different number of damper windings, are critically assessed. The simulations are carried out using frequency responses and step voltage responses.

Keywords: SVC, Small-Signal Stability, Block Diagram Models, Multi-Machine System.

1. Introduction

In small-signal stability applications, the state-space and block diagram approaches have been used for many years [1]. The eigenvalue-based, state-space techniques have the ability to solve large-scale power systems, relying heavily on mathematical abstraction. On the other hand, the block diagram approach provides a physical-oriented way of conducting dynamic analysis of power systems but, so far, it has been deemed to be only applicable to small-scale power systems. For instance, a transfer-function block diagram model [2-4] has been used to study the dynamic behaviour of a synchronous generator feeding into an infinite-bus via a tie-line system. The method captures the essence of how the AVR interacts physically with the generator through its main field winding. Also, a block diagram model [5] has been used to look at the dynamic interactions of two machines and their excitation control systems.

With the advent of Flexible AC Transmission Systems (FACTS) equipment, which has the capability to provide fast-acting active and reactive power control to high-voltage networks, the study of the impact of FACTS devices on power system dynamics has become a topic of great research importance. A great deal of progress has been achieved in incorporating FACTS device models into the state-space representation form [6-8]. One possible reason for the popularity of this approach is that the addition of new power plant component models into the standard state-space model of the power network is quite a straightforward endeavour. In contrast, owing to the large and very detailed amount of analytical work associated with the incorporation of new power plant models into the block-diagram approach, only a limited amount of progress has been achieved with this method. Nevertheless, owing to the great advantages that the method has in yielding physical insight, we feel that further development of this method should be pursued.

We are not alone in this belief and a block diagram model, including a number of the FACTS devices, has been proposed for the study of single-machine systems and their interaction with FACTS devices [9]. Furthermore, a unified model including multiple generators and FACTS devices has been presented more recently [10]. However, these models exhibit some very serious short-comings since only the generator main field winding is represented. Hence, the model may not always yield realistic dynamic

responses. Moreover, the dynamic interactions between SVC controllers and the power system have not been fully implemented. For instance, the SVC dynamic voltage is not included in the voltage control loop. Bearing this in mind, this author has embarked on the development of a more advanced multi-machine and multi-FACTS block diagram model than that reported in [10]. The incorporation of the SVC model in this generic frame-of-reference has been successfully completed. Hence, the author would like to report on the case of the multi-machine, multi-SVC system.

The block diagram models developed cater for a different number of machine damper windings: (i) one damper winding along the *d*- and *q*-axes. (ii) one damper winding along the *q*-axis and (iii) no damper windings. The dynamic performances of the various system models are critically evaluated in order to assess the reliability of damper winding representation on small-signal stability. A small-scale power system consisting of two machines and one SVC, is taken as the base case study in order to capture comprehensively all relevant aspects of system dynamics. The system is then expanded to encompass two SVC systems.

2. System and Block Diagram Model Representations

To study the dynamic interactions between generators and SVCs in a multi-machine environment, a linearised transfer-function which caters for n generators and m SVCs is developed. Full derivations of the transfer functions for the i^{th} machine and the i^{th} SVC are given in Appendix A. After suitable manipulations, the linearised expressions, in the s domain, lead to three models with a varying degree of complexity.

Model 1: This model accounts for the effect of the generator main field plus one damper winding in the *d*-axis and one in the *q*-axis.

$$\Delta P_{ei} = K_{1ii}\Delta\delta_i + \sum_{j\neq i}^{n} K_{1ij}\Delta\delta_j + K_{2ii}\Delta E''_{qi} + \sum_{j\neq i}^{n} K_{2ij}\Delta E''_{qj} + K_{2dii}\Delta E''_{di} + \sum_{j\neq i}^{n} K_{2dij}\Delta E''_{dj} + K_{svc1ii}\Delta\alpha_i + \sum_{j\neq i}^{m} K_{svc1ij}\Delta\alpha_j \quad (1)$$

$$\Delta e_{ti} = K_{5ii}\Delta\delta_i + \sum_{j\neq i}^{n} K_{5ij}\Delta\delta_j + K_{6ii}\Delta E''_{qi} + \sum_{j\neq i}^{n} K_{6ij}\Delta E''_{qj} + K_{6dii}\Delta E''_{di} + \sum_{j\neq i}^{n} K_{6dij}\Delta E''_{dj} + K_{svc3ii}\Delta\alpha_i + \sum_{j\neq i}^{m} K_{svc3ij}\Delta\alpha_j \quad (2)$$

$$\Delta V_{svci} = K_{5nii}\Delta\delta_i + \sum_{j\neq i}^{n} K_{5nij}\Delta\delta_j + K_{6nii}\Delta E''_{qi} + \sum_{j\neq i}^{n} K_{6nij}\Delta E''_{qi} + K_{6dnii}\Delta E''_{di} + \sum_{j\neq i}^{n} K_{6dnij}\Delta E''_{di} + K_{svc3nii}\Delta\alpha_i + \sum_{j\neq i}^{m} K_{svc3nij}\Delta\alpha_j \quad (3)$$

where

$$\Delta E''_{qi} = g_{3ii}(S)\Delta E_{fdi} - \sum_{j\neq i}^{n} g_{3ij}(S)\Delta E''_{qj} - g_{4ii}(S)\Delta\delta_i - \sum_{j\neq i}^{n} g_{4ij}(S)\Delta\delta_j - g_{7ii}(S)\Delta E''_{di} - \sum_{j\neq i}^{n} g_{7ij}(S)\Delta E''_{dj} - g_{svc2ii}(S)\Delta\alpha_i - \sum_{j\neq i}^{m} g_{svc2ij}(S)\Delta\alpha_j \quad (4)$$

$$\Delta E''_{di} = \sum_{j\neq i}^{n} g_{7dij}(S)\Delta E''_{dj} + g_{4dii}(S)\Delta\delta_i + \sum_{j\neq i}^{n} g_{4dij}(S)\Delta\delta_j + g_{3dii}(S)\Delta E''_{qi} + \sum_{j\neq i}^{n} g_{3dij}(S)\Delta E''_{qj} + g_{svc2dii}(S)\Delta\alpha_i + \sum_{j\neq i}^{m} g_{svc2dij}(S)\Delta\alpha_j \quad (5)$$

The coefficients and transfer functions in (1)-(5) are given in Appendix A.

Model 2: In this model the damper winding in the *d*-axis rotor circuit is removed from Model 1. Hence, $\Delta E''_q$ and X''_d in (1)-(5) are replaced by $\Delta E'_q$ and X'_d, respectively.

Model 3: In this model both damper windings are neglected. Hence, only the effect of the field winding, $\Delta E'_q$, exists, i.e. $\Delta E''_q = \Delta E''_d = X''_d = X''_q = 0$.

The generic block diagram model, shown in Fig. 1, for the i^{th} machine and the i^{th} SVC and contributions from the j^{th} generator and the j^{th} SVC is derived from (1)-(5). The sub-blocks enclosed by the dotted line are the coefficients of the i^{th} machine. The dynamic characteristic of the i^{th} machine is suitably represented by incremental changes in four main variables, namely output power (ΔP_{ei}), output voltage (Δe_{ti}), voltages proportional to *d*- and *q*-axes flux linkages ($\Delta E''_{qi}$) and ($\Delta E''_{di}$), respectively. The dynamic contributions from the j^{th} generator consists of a summation of changes in $\Delta\delta_j$, $\Delta E''_{qj}$ and $\Delta E''_{dj}$, inputted through the coefficients with subscripts ij, where j=1...n and $j\neq i$. These contributions are delivered to the generic block diagram model of the i^{th} machine.

As shown in Fig. 1, the dot-dot-dashed line block encloses the i^{th} SVC system. It can be seen that the i^{th} SVC terminal voltage (ΔV_{svci}) is made up of changes in $\Delta\delta$, $\Delta E''_q$ and $\Delta E''_d$ through the coefficients K_{5n}, K_{6n} and K_{6dn}.

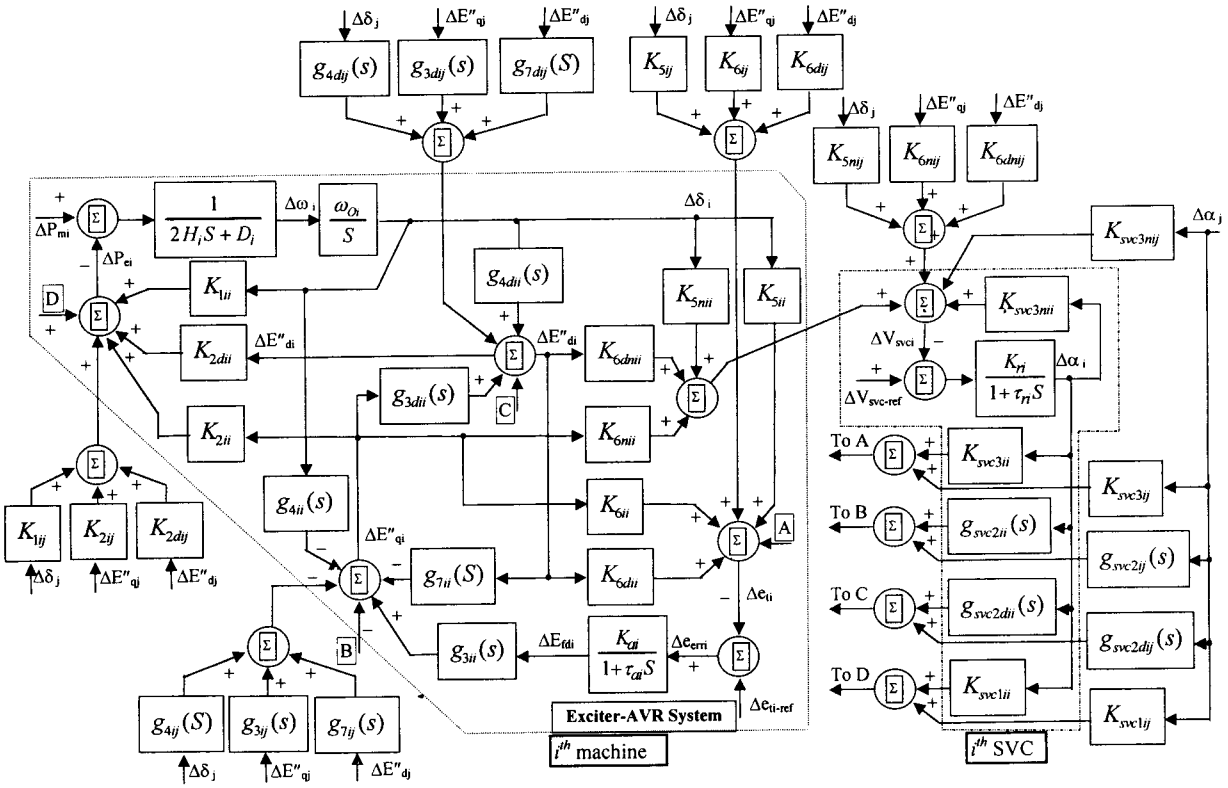

Fig. 1 Block diagram of the i^{th} machine and the i^{th} SVC in a multi-machine system

The changes contributed by the i^{th} and j^{th} machines are combined and fed into the i^{th} SVC voltage controller. The terminal voltage of the i^{th} SVC is also determined by changes in its firing angle ($\Delta\alpha_i$) through the coefficient $K_{svc3nii}$ and by a summation of changes in the j^{th} SVC's firing angle ($\Delta\alpha_j$) through the coefficients $K_{svc3nij}$, where $j=1\ldots m$, and $j\neq i$. A change in $\Delta\alpha_j$ through the coefficient $K_{svc3nij}$ reflects a dynamic interaction between the i^{th} and j^{th} SVCs. The combined impact of the m SVCs is inputted at the summing points A, B, C and D, respectively. These contributions are added to changes in Δe_{ti}, $\Delta E''_{qi}$, $\Delta E''_{di}$ and ΔP_{ei} of the i^{th} machine through the existing connections between the generator and the SVC at points A, B, C and D, respectively.

It can be seen from the i^{th} machine model that changes in Δe_{ti} and ΔP_{ei} are mainly determined by variations in $\Delta E''_{qi}$ and $\Delta E''_{di}$. Since damper windings in both the d- and q-axes are accounted for, there is an additional dynamic loop formed by these flux linkages inside each machine, via the transfer functions $g_7(s)$ and $g_{3d}(s)$. It should be noticed that the existence of $g_7(s)$ and $g_{3d}(s)$ is due to the more realistic conditions being considered in this analysis, such as the resistive part of transmission lines impedances and the explicit representation of PQ loads. Also, the subtransient saliency, i.e., $X''_d \neq X''_q$, plays an important part in the existence of these transfer functions. Referring to (4), it can be seen that the transfer functions making up $\Delta E''_{qi}$ have the same time constants, but different gains. A similar situation arises for $\Delta E''_{di}$ in (5).

In power system operation, the machine damper windings play a crucial role in providing system damping. It can be seen from Fig. 1 that changes in $\Delta E''_{qi}$ and $\Delta E''_{di}$ will be influenced by the d- and q-axes damper windings, respectively. Also, the flux linkage between the d- and q-axes within the i^{th} machine will also interact dynamically with those of other

machines and with the SVCs. Therefore, if the generator damper windings effects are neglected, as they have been in [9-10], it will lead to a system model with unrealistic system damping. In the section below, an assessment of the various system models, with decreasing order of machine modelling, is carried out.

3. Assessment of Block Diagram Models

3.1. Synchronous generator interaction

The impact of neglecting machine damper windings on system model integrity is assessed in this section. The two-machine system shown in Fig. 2, but with no SVC in node 3, is used in this study. Machine 2 is represented by Models 1-3 whereas machine 1 is always represented by Model 1. The open-loop frequency responses of Machines 1 and 2 are studied in order to gain insight into the effect of neglecting damper windings. It is noted that the open-loop frequency response Δe_{ti} /Δe_{erri} of one of the machines is obtained while the other machine is kept in close-loop control with the fast-acting voltage regulator (AVR). The system parameters are given in Table B1 and system operating conditions are given in Table B2.

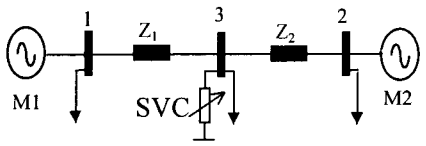

Fig. 2 Two generator one-SVC system

Figs. 3 and 4 show the open-loop frequency responses of machines 1 and 2, respectively. It can be seen from Fig. 4 that when Model 2 is used to represent machine 2, its frequency response shows a reduction in phase lead with respect to the case when Model 1 is used to represent machine 2. The reduction starts at the natural oscillation frequency and results are shown up to 100 rad/s. As expected, machine 2 represented by Model 1 exhibits better dynamic performances in these frequency ranges than those of machine 2 with Model 2. The effect of using Model 2 for machine 2 is passed on to machine 1. It can be seen from Fig. 3 that this effect causes a slight change in machine 1's characteristic. When Model 3 is applied to represent machine 2, the frequency response in Fig. 4 shows that machine 2 is unstable,

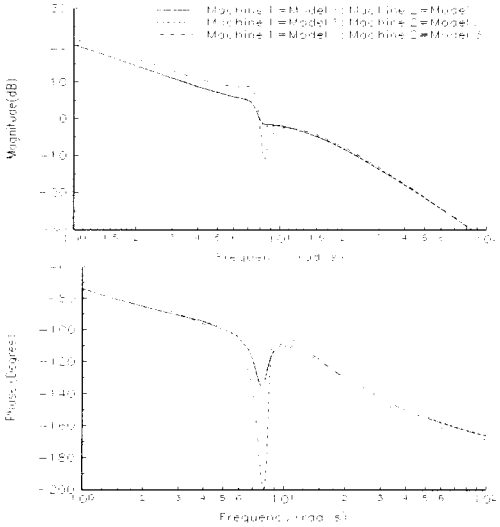

Fig. 3 Open-loop frequency response of machine 1

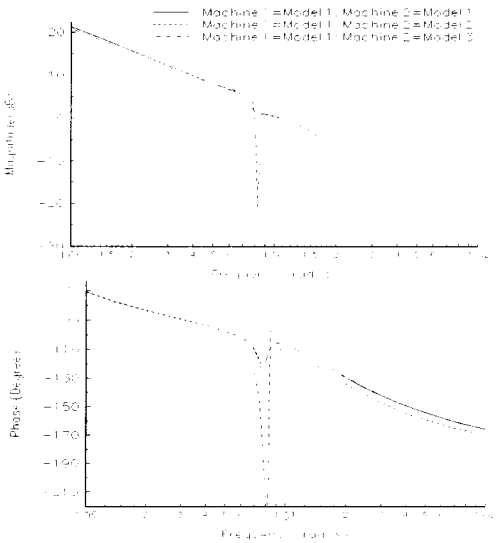

Fig. 4 Open-loop frequency response of machine 2

exhibiting a very pronounced switch-back characteristic due to the lack of realistic system damping. In this exercise, and for the purpose of results presentation, a damping term D=12.5 was applied at the mechanical mode of machine 2. The effect of using Model 3 to represent machine 2 also introduces an undamped response, with a high switch-back characteristic into the frequency response of machine 1, represented by Model 1. It can be concluded that neglecting the damping windings of machines has a very significant degrading effect on the generator dynamic response characteristic in small-signal stability studies.

3.2 Synchronous generator-SVC interactions

In order to assess the overall dynamic characteristic of the system model shown in Fig. 1, the SVC at node 3 is set to supply 0.357 p.u. reactive power. Hence, the voltage magnitude at node 3 increases from 0.928 to 0.98 p.u. The system parameters and operating conditions are given in Tables B1 and B2, respectively. Three different cases are analysed below: Model 1 is used to represent machines 1 and 2, this is followed by the use of Model 2 and then Model 3. It should be noted that for the first two cases the mechanical damping term D of both machines is set to zero whereas for the third case D=9.75.

Fig. 5 shows plots of gain and phase versus frequency for machine 1. In this case, a high value of mechanical damping, D=9.75, is applied to Model 3 in order to provide a similar amount of phase than Model 1, at the switch-back frequency point. It should be noted that a severely undamped response would take place if zero mechanical damping were to be used in Model 3. When Model 2 is employed the system damping is significantly improved over the frequency range of concern, without having to resort to artificially high levels of mechanical damping. Nevertheless, when compared to Model 1, Model 2 has approximately a 10° lower phase lead at the natural oscillation frequency. This indicates that Model 2 has indeed lower damping. The phase of Model 2 is also lower than that of Model 1, starting at the natural oscillation frequency. Therefore, Model 1 with generator damper windings in the *d*- and *q*-axes provides a better frequency performance than Models 2 and 3, particularly at the high frequency range.

The time responses in Figs. 6 and 7 can also be used quite effectively to show the impact of damper winding representation in system model. Even though lack of inherent damping in Model 3 is compensated in this paper by adding artificial mechanical damping, Fig. 6 reveals that the voltage time response obtained from Model 3 has a different frequency of oscillation than that of Model 1. On the other hand, Fig. 7 shows that the oscillation frequency in the voltage time response of Model 2 is closer to the response of Model 1 than that of Model 3. However, the time response of Model 2 has a different oscillatory magnitude than Model 1 and it also reaches the steady state at a slightly later time. It should be said that neglecting both machine damper windings, i.e. Model 3, is not a suitable option for carrying out small-signal stability analysis. Although adding the q-axis damper winding, i.e. Model 2, improves significantly the reliability of system model response, including damper windings in both the *d*- and *q*-axes leads to an even better reliability of system model response.

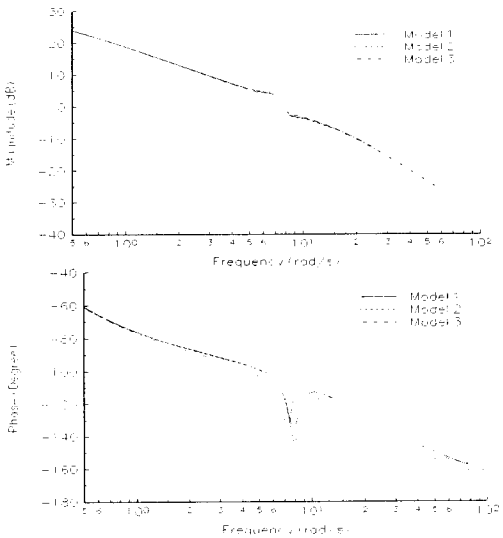

Fig. 5 Frequency response of machine 1 with differing order of system models

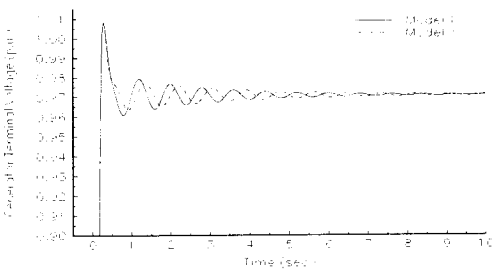

Fig. 6 Machine 1's terminal voltage for Models 1 and 3

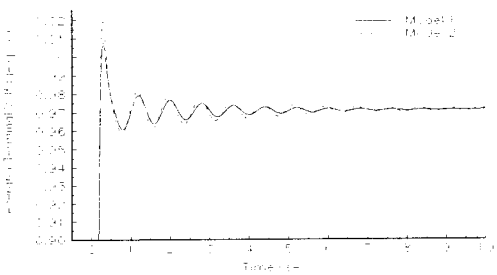

Fig. 7 Machine 1's terminal voltage for Models 1 and 2

4. Multi-machine Study Case

Having established the suitability of Model 1 in small-signal stability studies, we now investigate the impact of SVC systems in a multi-machine, multi-SVC environment. The two machine system shown in Fig. 8 is used together with the system parameters and operating conditions given in Tables B1 and B3, respectively. The frequency response of generators 1 and 2 with SVCs and with no SVCs are shown in Fig. 9 and 10. Similarly, their voltage responses are shown in Fig. 11 and 12.

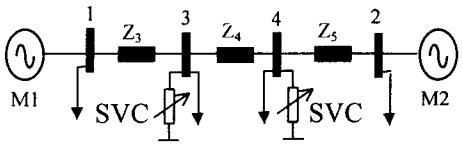

Fig. 8 Two-generators Two-SVCs system

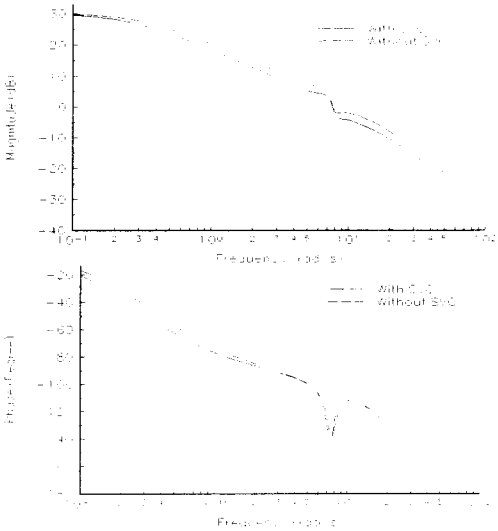

Fig. 9 Frequency response of machine 1

The plots of gain and phase versus frequency for both machines are shown in Figs. 9 and 10. The switch-back characteristics clearly show that machine 1 has a lower damping response at the natural oscillation frequency than machine 2. This is an expected result since machine 1 supplies a heavier active load than machine 2, as illustrated in Table B3. The frequency responses also show that the SVCs only provide a slight damping improvement to machine 1 at the natural oscillation frequency. However, the SVCs enhance the high frequency performance of both machines, where higher phase leads can be observed at frequencies above 11 rad/s.

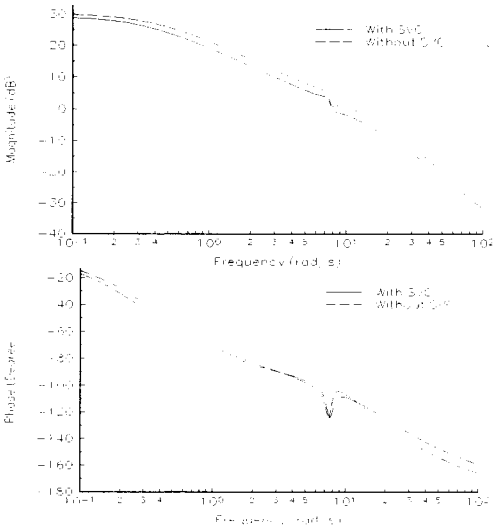

Fig. 10 Frequency response of machine 2

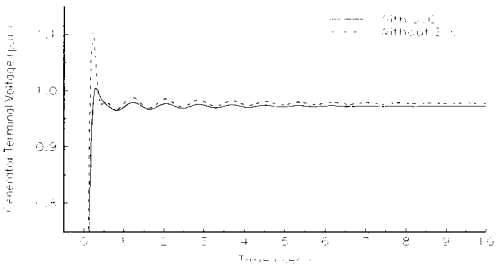

Fig. 11 Voltage response of machine 1

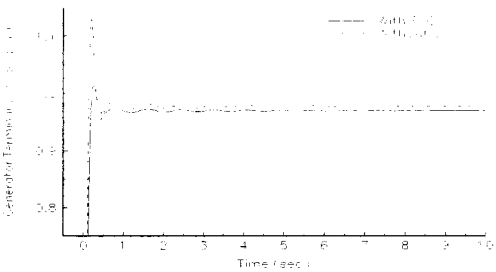

Fig. 12 Voltage response of machine 2

Also, the time voltage responses in Figs. 11 and 12 show that the SVCs reduce the first peak of oscillation in the generator output voltage when a step change in the AVR reference voltage ($\Delta e_{ti\text{-}ref}$) is applied. However, the frequency responses illustrate that the SVCs are

responsible for a slight reduction in the steady-state gains of the system, causing the generator output voltages to reach a slightly lower steady-state levels. It should be noticed that the same amount of PQ load is used in both cases, when the system contains SVCs and no SVCs.

5. Conclusions

The block diagram model of a multi-machine and multi-SVC system is presented in this paper. In this simulation environment full dynamic interactions between generators and SVCs are accounted for. The model allows for a good explanation of how the SVCs impact on the generator dynamic characteristics. Assessment of the dynamic performance of the i^{th} machine indicates that its dynamic performance is severely impaired if the damper winding effects are neglected in the study. The results presented in the paper show that model reliability critically depends on including one or two damper windings. Hence, it is recommended that Model 1 should become the standard machine model in small-signal stability studies. This should ensure that system model reliability is maintained in small-signal stability studies of multi-machine systems with excitation control and FACT devices.

6. References

[1] Kundur, P., Power System Stability, McGraw-Hill Inc, 1993.

[2] Heffron, W.G. and Phillips, R.A., Effect of Modern Amplidyne Voltage Regulator Characteristics, *AIEE Trans. on Power App. and Systems*, Vol. PAS-71, Aug, pp. 692-697, 1952.

[3] Demello, F.P. and Concordia, C., Concepts of Synchronous Machine Stability as Affected by Excitation Control, *IEEE Trans. on Power App. and Systems*, Vol. PAS-88, No. 4, April, pp. 189-202, 1969.

[4] Saidy, M. and Hughes, F. M., Block Diagram Transfer Function Model of a Generator Including Damper Windings, *IEE Proc.- Gen. Trans. Distrib.*, Vol. 141, No. 6, Nov, pp. 599-608, 1994.

[5] Moussa, H. A M. and Yao-nan, Yu., Dynamic Interaction of Multi-machine Power System and Excitation Control, *IEEE Trans. on Power App. and Systems*, Vol. PAS-93, No. 4, July, pp. 1150-1158, 1974.

[6] Arabi, S., Rogers, G.J., Wong, D.Y., Kundur, P. and Lauby, M.G., Small Signal Stability Program Analysis of SVC and HVDC in AC Power Systems, *IEEE Trans. on Power Systems*, Vol. 6, No. 3, August, pp. 1147-1153, 1991.

[7] Padiyar, K. R., Varma, R. K., Damping Torque Analysis of Static Var System Controller, *IEEE Trans. on Power Systems*, Vol. 6, No. 2, May, pp. 458-465, 1991.

[8] Tang, Y., Meliopoulos, A. P. S., Power System Small Signal Stability Analysis with FACTS Elements, IEEE Trans. on Power Delivery, Vol. 12, No. 3, July, pp 1353-1361, 1997.

[9] Wang, H.F. and Swift, F. J., A Unified Model for the Analysis of FACTS Devices in Damping Power System Oscillation Part I: Single-machine Infinite-bus Power System, *IEEE Trans. on Power Delivery*, Vol. 12, No. 12, April, pp. 941-946, 1997.

[10] Wang, H.F., Swift, F. J. and Li, M., A Unified Model for the Analysis of FACTS Devices in Damping Power System Oscillation Part II: Multi-machine Power System, *IEEE Trans. on Power Delivery*, Vol. 13, No. 4, October, pp. 1355-1362, 1998.

[11] IEEE Strandard, IEEE Guide for Synchronous Generator Modelling Practices in Stability Analyses, 1110-1991.

[12] Dandeno, P. L., Hauth, R. L., Effect of Synchronous Machine Modelling in Large Scale System Studies, *IEEE Trans. on Power App. and Systems*, Vol. PAS-92, No. 2, March, pp. 574-582, 1973.

[13] IEEE COMMITTEE REPORT, Current Usage and Suggested Practices in Power System Stability Simulation for Synchronous Generator Machines, *IEEE Trans. on Energy Conversion*, Vol. EC-1, No. 1, March, pp. 77-93, 1986.

[14] Shaltout, A. A., Robert, T. H., Analysis of Damping and Synchronising Torques, *IEEE Trans. on Power App. and Systems*, Vol. PAS-98, September, pp. 1701-1705, 1979.

[15] Torseng, S., Shunt Connected Reactor and Capacitors Controlled by Thyristors, *IEE Proc, Gen Trans. & Distrib*, Vol. 128, November, pp. 366-373, 1981.

[16] Dandeno, P. L., Kundur, P., Poray, A. T., Zein, H. M., El-Din Adaptation and Validation of Turbogenerator Model Parameter Through On-Line Frequency Response Measurements, *IEEE Trans. on Power App. and Systems*, Vol. PAS-100, No. 4, April, pp. 1656-1662, 1981.

[17] Zhou, E.Z., Application of Static Var Conpensators to Increase Power System Damping, *IEEE Trans. on Power Systems*, Vol. 8, No. 2, May, pp. 655-661, 1993.

[18] Ho, P.T. and Tso, S.K., Software Control of Static Reactive Current Compensator, *IEE Proc, Gen Trans. & Distrib*, Vol. 135, No. 6, Nov, pp. 518-527, 1988.

Appendix A1

The admittance matrix for n-generator nodes plus m-SVC nodes can be expressed as,

$$\begin{bmatrix} [\vec{I}_g] \\ 0 \end{bmatrix} = \begin{bmatrix} [\vec{Y}_{nn}] & [\vec{Y}_{nm}] \\ [\vec{Y}_{mn}] & [\vec{Y}_{mm}]+[\vec{Y}_{svc}] \end{bmatrix} \begin{bmatrix} [\vec{E}_t] \\ [\vec{V}_{svc}] \end{bmatrix} \quad \text{(A-1)}$$

where

$$[\vec{Y}_{svc}] = j\left[X_C - K\{(\pi-\alpha)+0.5Sin(2\alpha)\}\right] \text{ and } K = \frac{2}{\pi X_L}$$

For a small change, the generator terminal voltages in *D-Q* network co-ordinates can be written as,

$$[\Delta\vec{E}_t] = [e^{j(\delta-\pi/2)}]\Big\{[\Delta\vec{E}''] + [X_q'' - X_d''][\Delta i_{gq}] + j\Big[[\vec{E}''] + [X_q'' - X_d''][i_{gq}]\Big][\Delta\delta]\Big\} - [jX_d''][\Delta\vec{I}_g] \quad \text{(A-2)}$$

After re-arranging (A-1) in term of small perturbations by making use of (A-2), the generator current of machines in *D-Q* co-ordinates can be expressed as,

$$[\Delta\vec{I}_g] = [\vec{Y}_g][e^{j(\delta-\pi/2)}]\Big\{[\Delta\vec{E}''] + [X_q'' - X_d''][\Delta i_{gq}] + j\Big[[\vec{E}''] + [X_q'' - X_d''][i_{gq}]\Big][\Delta\delta]\Big\} - [\vec{Y}_s][\Delta\vec{Y}_{svc}][\vec{V}_{svc}] \quad \text{(A-3)}$$

where

$$[\vec{Y}_g] = \left[[\vec{Y}_a]^{-1} + j[X_d'']\right]^{-1}$$

$$[\vec{Y}_s] = [\vec{Y}_g][\vec{Y}_a]^{-1}[\vec{Y}_{nm}][\vec{Y}_{mm} + \vec{Y}_{svc}]^{-1}$$

$$[\vec{Y}_a] = [\vec{Y}_{nn}] - [\vec{Y}_{nm}][\vec{Y}_{mm} + \vec{Y}_{svc}]^{-1}[\vec{Y}_{mn}]$$

$$[\Delta\vec{Y}_{svc}] = j[(K - K\cdot Cos(2\alpha))\cdot\Delta\alpha]$$

It should be noted that the non-linear term of $\Delta\vec{Y}_{svc}$ is cancelled out by an ideal linearised block in the SVC model [6]. So, $[\Delta\vec{Y}_{svc}] = j[K\Delta\alpha]$

Re-arranging (A-3), the current of i^{th} machine in d_i-q_i machine co-ordinates is given by,

$$\Delta\vec{i}_{gi} = \sum_{j=1}^{n} \vec{Y}_{gij} e^{j\delta_{ji}} \Big\{\Delta\vec{E}_j'' + (X_{qj}'' - X_{dj}'')\Delta i_{gqj} + j\Big(\vec{E}_j'' + (X_{qj}'' - X_{dj}'')i_{gqj}\Big)\Delta\delta_{ji}\Big\} - \sum_{j=1}^{m} \vec{Y}_{sij} e^{j(-\delta_i+\pi/2)}(jK_j)\vec{V}_{svcj}\Delta\alpha_j \quad \text{(A-4)}$$

where $\delta_{ji} = \delta_j - \delta_i$ $\quad \Delta\delta_{ji} = \Delta\delta_j - \Delta\delta_i$

Decomposing (A-4) in *d* an *q*-axes give,

$$[\Delta i_{gd}] = [D_d][\Delta E_q''] + [Q_d][\Delta E_d''] + [R_d][\Delta\delta] + [A_d][\Delta\alpha] \quad \text{(A-5)}$$

$$[\Delta i_{gq}] = [D_q][\Delta E_q''] + [Q_q][\Delta E_d''] + [R_q][\Delta\delta] + [A_q][\Delta\alpha] \quad \text{(A-6)}$$

where

$$[R_q] = [C_{Qq}]^{-1}[K_{Rq}] \qquad [D_q] = [C_{Qq}]^{-1}[K_{Dq}]$$

$$[Q_q] = [C_{Qq}]^{-1}[K_{Qq}] \qquad [A_q] = [C_{Qq}]^{-1}[K_{Aq}]$$

$$[R_d] = [K_{Rd}] + [C_{Qd}][R_q] \qquad [D_d] = [K_{Dd}] + [C_{Qd}][D_q]$$

$$[Q_d] = [K_{Qd}] + [C_{Qd}][Q_q] \qquad [A_d] = [K_{Ad}] + [C_{Qd}][A_q]$$

$$K_{Rdij} = -Y_{gij}\left\{C_{gij}E_{qj}'' + S_{gij}(E_{dj}'' + (X_{qj}'' - X_{dj}'')i_{gqj})\right\} \quad \text{for } j\neq i$$

$$K_{Rqij} = -Y_{gij}\left\{S_{gij}E_{qj}'' - C_{gij}(E_{dj}'' - (X_{qj}'' - X_{dj}'')i_{gqj})\right\} \quad \text{for } j\neq i$$

$$K_{Rdii} = -\sum_{j\neq i}^{n} K_{Rdij} \qquad K_{Rqii} = -\sum_{j\neq i}^{n} K_{Rqij}$$

$$K_{Ddij} = -Y_{gij}S_{gij} \qquad K_{Dqij} = Y_{gij}C_{gij} \quad \text{for } j=1\rightarrow n$$

$$K_{Qdij} = Y_{gij}C_{gij} \qquad K_{Qqij} = Y_{gij}S_{gij} \quad \text{for } j=1\rightarrow n$$

$$C_{Qdij} = Y_{gij}C_{gij}(X_{qj}'' - X_{dj}'') \qquad \text{for } j=1\rightarrow n$$

$$C_{Qqij} = -Y_{gij}S_{gij}(X_{qj}'' - X_{dj}'') \text{ for } j\neq i \quad C_{Qqii} = 1 + C_{Qqii} \text{ for } j=i$$

$$K_{Adij} = Y_{sij}B_{ij}K_j \qquad K_{Aqij} = Y_{sij}A_{ij}K_j \quad \text{for } j=1\rightarrow m$$

$$\vec{Y}_{gij} = Y_{gij}e^{j\beta_{ij}} \qquad \vec{Y}_{sij} = Y_{sij}e^{j\gamma_{ij}}$$

$$C_{gij} = Cos(\delta_{ji} + \beta_{ij}) \qquad S_{gij} = Sin(\delta_{ji} + \beta_{ij})$$

$$C_{sij} = Cos(\delta_i + \gamma_{ij}) \qquad S_{sij} = Sin(\delta_i + \gamma_{ij})$$

$$A_{ij} = S_{sij}V_{svcdj} + C_{sij}V_{svcqj} \qquad B_{ij} = C_{sij}V_{svcdj} - S_{sij}V_{svcqj}$$

Electrical power equation:

The electrical power of the generators can be expressed as,

$$[P_e] = [E_d''][i_{gd}] + [E_q''][i_{gq}] + [i_{gq}][X_q'' - X_d''][i_{gd}] \quad \text{(A-7)}$$

After re-arranging (A-7) in term of small variations by making use of (A-5)-(A-6), equation (1) in the main body of the paper is obtained, where

$$K_{1ii} = P_Q R_{qii} + P_D R_{dii} \qquad K_{1ij} = P_Q R_{qij} + P_D R_{dij}$$

$$K_{2ii} = i_{qi} + P_{Qi} D_{qii} + P_D D_{dii} \qquad K_{2ij} = P_Q D_{qij} + P_D D_{dij}$$

$$K_{2dii} = i_{di} + P_Q Q_{qii} + P_D Q_{dii} \qquad K_{2dij} = P_Q Q_{qij} + P_D Q_{dij}$$

$$K_{svc1ii} = P_Q A_{qii} + P_D A_{dii} \qquad K_{svc1ij} = P_Q A_{qij} + P_D A_{dij}$$

$$P_D = E_{di}'' + (X_{qi}'' - X_{di}'')i_{qi} \qquad P_Q = E_{qi}'' + (X_{qi}'' - X_{di}'')i_{di}$$

D-axis flux linkage equation:

The *d*-axis flux linkage generated by the main field and one *d*-axis damper windings can be written in matrix form as,

$$[C_3(S)][\Delta E_q''] = [C_1(S)][\Delta E_{fd}] - [C_2(S)][\Delta i_{gd}] \quad \text{(A-8)}$$

$$[C_1(S)] = \left[[1] + [\tau_{do}'']S\right]$$

$$[C_3(S)] = \left[[1] + [\tau_{do}' + \tau_{do}'']S + [\tau_{do}'\tau_{do}'']S^2\right]$$

$$[C_2(S)] = \left[[X_d - X''_d] + \left[\tau'_{do}[X'_d - X''_d] + \tau''_{do}[X_d - X'_d]\right]S\right]$$

After re-arranging (A-8) by making use of (A-5), equation (4) in the main body of the paper is obtained, where

$$g_{3ii}(S) = \frac{1+\tau''_{doi}S}{\Delta(S)} \qquad g_{3ij}(S) = \frac{\Theta(S)}{\Delta(S)} D_{dij}$$

$$g_{4ii}(S) = \frac{\Theta(S)}{\Delta(S)} R_{dii} \qquad g_{4ij}(S) = \frac{\Theta(S)}{\Delta(S)} R_{dij}$$

$$g_{7ii}(S) = \frac{\Theta(S)}{\Delta(S)} Q_{dii} \qquad g_{7ij}(S) = \frac{\Theta(S)}{\Delta(S)} Q_{dij}$$

$$g_{svc2ii}(S) = \frac{\Theta(S)}{\Delta(S)} A_{dii} \qquad g_{svc2ij}(S) = \frac{\Theta(S)}{\Delta(S)} A_{dij}$$

$$\Theta(S) = \left\{X_{di} - X''_{di}\right\} + \left\{\tau'_{doi}(X'_{di} - X''_{di}) + \tau''_{doi}(X_{di} - X'_{oi})\right\}S$$

$$\Delta(S) = \left\{1 + (X_{di} - X''_{di})D_{dii}\right\} + \left\{\left(\tau'_{doi}(X'_{di} - X''_{di}) + \tau''_{doi}(X_{di} - X'_{di})\right)D_{dii} + (\tau'_{doi} + \tau''_{doi})\right\}S + \left\{\tau'_{doi}\tau''_{doi}\right\}S^2$$

Q-axis flux linkage equation:

The flux linkage given by one q-axis damper winding can be written in matrix form as,

$$\left[[1] + [\tau''_{qo}]S\right][\Delta E''_d] = [X_q - X''_q][\Delta i_{gq}] \qquad \text{(A-9)}$$

After re-arranging (A-9) by making use of (A-6), equation (5) in the main body of the paper is obtained, where

$$g_{3dii}(S) = \Omega(S)D_{qii} \qquad g_{3dij}(S) = \Omega(S)D_{qij}$$

$$g_{4dii}(S) = \Omega(S)R_{qii} \qquad g_{4dij}(S) = \Omega(S)R_{qij}$$

$$g_{svc2dii}(S) = \Omega(S)A_{qii} \qquad g_{svc2dij}(S) = \Omega(S)A_{qij}$$

$$g_{7dij}(S) = \Omega(S)Q_{qij} \quad \Omega(S) = \frac{(X_{qi} - X''_{qi})}{1 - (X_{qi} - X''_{qi})Q_{qii} + \tau''_{qoi}S}$$

Generator terminal voltage equation:

For small variations, the generator terminal voltage can be written in matrix form for n machine as,

$$[\Delta e_t] = [e_t]^{-1}\left[[e_{td}][\Delta e_{td}] + [e_{tq}][\Delta e_{tq}]\right] \qquad \text{(A-10)}$$

After suitable manipulation of (A-10), equation (2) in the main body of the paper is obtained, where

$$K_{5ii} = E_D X''_{qi} R_{qii} - E_Q X''_{di} R_{dii}$$

$$K_{5ij} = E_D X''_{qi} R_{qij} - E_Q X''_{di} R_{dij}$$

$$K_{6ii} = E_D X''_{qi} D_{qii} + E_Q(1 - X''_{di})D_{dii}$$

$$K_{6ij} = E_D X''_{qi} D_{qij} - E_Q X''_{di} D_{dij}$$

$$K_{6dii} = E_D(1 + X''_{qi})Q_{qii} - E_Q X''_{di} Q_{dii}$$

$$K_{6dij} = E_D X''_{qi} Q_{qij} - E_Q X''_{di} Q_{dij}$$

$$K_{svc3ii} = E_D X''_{qi} A_{qii} - E_Q X''_{di} A_{dii}$$

$$K_{svc3ij} = E_D X''_{qi} A_{qij} - E_Q X''_{di} A_{dij}$$

$$E_D = e_{ti}^{-1} e_{tdi} \quad E_Q = e_{ti}^{-1} e_{tqi}$$

SVC terminal voltage equation:

For small variations, the SVC voltage can be written in matrix form for m SVCs,

$$[\Delta V_{svc}] = [V_{svc}]^{-1}\left[[V_{svcD}][\Delta V_{svcD}] + [V_{svcQ}][\Delta V_{svcQ}]\right] \qquad \text{(A-11)}$$

Re-arranging (A-1) by making use of (A-2), the voltage of the i^{th} SVC in D-Q co-ordinates is given by,

$$\Delta\bar{V}_{svci} = -\sum_{j=1}^{n} \bar{Y}_{eij} e^{j(\delta_j - \pi/2)}\left(\Delta\bar{E}''_j + (X''_{qj} - X''_{dj})\Delta i_{gqj} + j\left(\bar{E}''_j + (X''_{qj} - X''_{dj})i_{gqj}\right)\Delta\delta_j\right) - \sum_{j=1}^{m} \bar{Y}_{dij}\Delta\bar{V}_{svcj}\bar{V}_{svcj} \qquad \text{(A-12)}$$

$$[\bar{Y}_e] = [\bar{Y}_d][\bar{Y}_{mn}][\bar{Y}_c][jX''_d]^{-1}$$

$$[\bar{Y}_d] = \left[[\bar{Y}_{mm} + \bar{Y}_{svc}] - [\bar{Y}_{mn}][\bar{Y}_c][\bar{Y}_{nm}]\right]^{-1}$$

$$[\bar{Y}_c] = \left[[jX''_d]^{-1} + [\bar{Y}_{nn}]\right]^{-1}$$

Decomposing (A-12) in D-Q co-ordinates gives,

$$[\Delta V_{svcD}] = [T_{Rd}][\Delta\delta] + [T_{Dd}][\Delta E''_q] + [T_{Qd}][\Delta E''_d] + [T_{Ad}][\Delta\alpha] \qquad \text{(A-13)}$$

$$[\Delta V_{svcQ}] = [T_{Rq}][\Delta\delta] + [T_{Dq}][\Delta E''_q] + [T_{Qq}][\Delta E''_d] + [T_{Aq}][\Delta\alpha] \qquad \text{(A-14)}$$

where

$$[T_{Rd}] = [S_{Rd}] + [S_{CQd}][R_q] \qquad [T_{Rq}] = [S_{Rq}] + [S_{CQq}][R_q]$$

$$[T_{Dd}] = [S_{Dd}] + [S_{CQd}][D_q] \qquad [T_{Dq}] = [S_{Dq}] + [S_{CQq}][D_q]$$

$$[T_{Qd}] = [S_{Qd}] + [S_{CQd}][Q_q] \qquad [T_{Qq}] = [S_{Qq}] + [S_{CQq}][Q_q]$$

$$[T_{Ad}] = [S_{Ad}] + [S_{CQd}][A_q] \qquad [T_{Aq}] = [S_{Aq}] + [S_{CQq}][A_q]$$

$$\bar{Y}_{eij} = Y_{eij} e^{j\theta_{ij}} \qquad \bar{Y}_{dij} = Y_{dij} e^{j\phi_{ij}}$$

$$S_{Rdij} = Y_{eij}\left(S_{fij}E''_{qj} - C_{fij}\left(E''_{dj} + (X''_{qj} - X''_{dj})i_{gqj}\right)\right) \text{ for } j=1\rightarrow n$$

$$S_{Rqij} = Y_{eij}\left(-C_{fij}E''_{qj} - S_{fij}\left(E''_{dj} + (X''_{qj} - X''_{dj})i_{gqj}\right)\right) \text{ for } j=1\rightarrow n$$

$$S_{Ddij} = -Y_{eij}C_{fij} \qquad S_{Dqij} = -Y_{eij}S_{fij} \text{ for } j=1\rightarrow n$$

$$S_{Qdij} = -Y_{eij}S_{fij} \qquad S_{Qqij} = Y_{eij}C_{fij} \text{ for } j=1\rightarrow n$$

$$S_{CQdij} = -Y_{eij}S_{fij}(X''_{qj} - X''_{dj}) \text{ for } j=1\rightarrow n$$

$$S_{CQqij} = Y_{eij}C_{fij}(X''_{qj} - X''_{dj}) \text{ for } j=1\rightarrow n$$

$$S_{Adij} = Y_{dij}a_{ij}K_j \qquad S_{Aqij} = -Y_{dij}b_{ij}K_j \qquad \text{for } j=1\rightarrow m$$

$$S_{fij} = Sin(\theta_{ij} + \delta_j)$$

$$a_{ij} = Sin(\phi_{ij})V_{svcDj} + Cos(\phi_{ij})V_{svcQj}$$

$$b_{ij} = Cos(\phi_{ij})V_{svcDj} - Sin(\phi_{ij})V_{svcQj}$$

Re-arranging (A-11) by making use of (A-13) and (A-14), equation (3) in the main body of the paper is obtained, where

$$K_{5nii} = V_D T_{Rdii} + V_Q T_{Rqii} \qquad K_{5nij} = V_D T_{Rdij} + V_Q T_{Rqij}$$

$$K_{6nii} = V_D T_{Ddii} + V_Q T_{Dqii} \qquad K_{6nij} = V_D T_{Ddij} + V_Q T_{Dqij}$$

$$K_{6dnii} = V_D T_{Qdii} + V_Q T_{Qqii} \qquad K_{6dnij} = V_D T_{Qdij} + V_Q T_{Qqij}$$

$$K_{svc3nii} = V_D T_{Adii} + V_Q T_{Aqii} \qquad K_{svc3nij} = V_D T_{Adij} + V_Q T_{Aqij}$$

$$V_D = V_{svci}^{-1} V_{svcDi} \qquad V_Q = V_{svci}^{-1} V_{svcQi}$$

Appendix B: System Operating Conditions and Parameters

	X_d	X'_d	X''_d	τ'_{do}	τ''_{do}	X_q	X''_q	τ''_{qo}	H	D
M1 and M2	1.445	0.316	0.179	5.26 s	0.028 s	0.959	0.162	0.159 s	4.27	0
	K_{a1}	K_{a2}	τ_{a1}	τ_{a2}						
AVR	100	115	0.05s	0.05s						
	Z_1	Z_2	Z_3	Z_4	Z_5					
Tie line Impedance	j0.25	j0.25	j0.2	j0.1	j0.2					
	K_r	X_L	X_C							
SVC1-SVC3	15	2.5	2.5							

Table B1 System parameters (All 100 MVA Base)

		V	Angle	$P_{injected}$	$Q_{injected}$	$P_{demanded}$	$Q_{demanded}$
Before applying SVC	Node 1	1.00000	0.0000	1.2	0.5338	0.60	0.2
	Node 2	1.0500	-0.4462	1.0	0.7557	0.40	0.2
	Node 3	0.9287	-9.2945	0.0	0.0	1.200	0.62
After applying SVC	Node 1	1.00000	0.0000	1.2	0.3262	0.60	0.2
	Node 2	1.0500	-0.4223	1.0	0.5380	0.40	0.2
	Node 3	0.98	-8.8044	0.0	0.3574	1.200	0.62

Table B2 System operating condition of system in Fig. 2

		V	Angle	$P_{injected}$	$Q_{injected}$	$P_{demanded}$	$Q_{demanded}$
Before applying SVC	Node 1	1.000	0.000	1.2	0.6727	0.30	0.1
	Node 2	1.000	-1.94	0.9	0.6056	0.20	0.1
	Node 3	0.9036	-11.49	0.0	0.0	1.00	0.4
	Node 4	0.9097	-10.79	0.0	0.0	0.6 0	0.3
After applying SVC	Node 1	1.000	0.000	1.2	0.2834	0.30	0.1
	Node 2	1.000	-1.77	0.9	0.2503	0.20	0.1
	Node 3	0.980	-10.58	0.0	0.3895	1. 00	0.4
	Node 4	0.980	-9.987	0.0	0.2538	0.60	0.3

Table B3 System operating condition of system in Fig. 8